Developmental and Comparative Immunology 148 (2023) 104915

Contents lists available at ScienceDirect

Developmental and Comparative Immunology

journal homepage: www.elsevier.com/locate/devcompimm

hnRNPM suppressed IRF7-mediated IFN signaling in the antiviral innate immunity in triploid hybrid fish

Huijuan Zhong [1], Qian Li [1], Shuaibin Pei, Yanfang Wu, Zhenghao Li, Xiaoyu Liu, Yuqing Peng, Tianle Zheng, Jun Xiao [*], Hao Feng [**]

State Key Laboratory of Developmental Biology of Freshwater Fish, College of Life Science, Hunan Normal University, Changsha, 410081, China

ARTICLE INFO

Keywords:
hnRNPM
IRF7
SVCV
Interferon
Triploid fish

ABSTRACT

Mammalian heterogeneous nuclear ribonucleoproteins M (hnRNPM) is a critical splicing regulatory protein that has been reported to negatively regulate the RLR signaling pathway by impairing the binding of RIG-I and MDA5 to viral RNA. To explore the role of hnRNPM in the antiviral innate immune response in teleost fish, the hnRNPM homologue of triploid fish (3nhnRNPM) has been cloned and identified in this paper. The CDS of *3nhnRNPM* gene is composed of 2016 nucleotides and encodes 671 amino acids. 3nhnRNPM migrated around 71 kDa in immunoblotting assay and was mainly detected in the nucleus in nucleo-cytoplasmic separation assay and immunofluorescent staining test. When 3nhnRNPM and 3nIRF7 were co-expressed in EPC cells, 3nhnRNPM significantly reduced the 3nIRF7-induced interferon (IFN) promoter transcription. Correspondingly, the mRNA levels of the SVCV-*M, -N, -P,* and *-G* genes were noteworthily enhanced, but the transcription levels of *epcIFNφ1*, *epcMx1*, *epcPKR*, and *epcISG15* were dramatically decreased. Additionally, the knockdown of 3nhnRNPM resulted in restricted SVCV replication and enhanced host cell antiviral activity. Furthermore, the association between 3nhnRNPM and 3nIRF7 has been identified by the co-immunoprecipitation assay. In addition, we found that 3nIRF7 was detained in the nucleus when co-expressed with 3nhnRNPM. To sum up, our data supported the conclusion that 3nhnRNPM suppressed 3nIRF7-mediated IFN signaling in the antiviral innate immunity.

1. Introduction

Vertebrates deploy their innate and adaptive immunity to resist the invasion of numerous harmful microorganisms. Teleost fishes, as the lower vertebrates, are more reliant on their innate immune system (Chen et al., 2017). The innate immune response is initiated when the pattern-recognition receptors (PRRs) recognize pathogen-associated molecular patterns (PAMPs). These PRRs include Toll-like receptors (TLRs), C-type lectin receptors, NOD-like receptors (NLRs), cytosolic DNA sensors, and retinoic acid-inducible gene I (RIG-I)-like receptors (RLRs) (Onomoto et al., 2021). RLRs are key RNA sensors in the cytosol, which consist of RIG-I, melanoma differentiation-associated gene 5 (MDA5), and laboratory of genetics and physiology 2 (LGP2) (Rehwinkel and Gack, 2020). RIG-I and MDA5 are activated by immunostimulatory RNA, for example, viral RNAs. LGP2 is believed to regulate RIG-I and MDA5 due to the lack of caspase activation and recruitment domains (CARDs) (Rehwinkel and Gack, 2020). Upon recognizing viruses, RIG-I and MDA5 recruit and activate the adaptor protein mitochondrial antiviral signaling (MAVS), and then further gathers and transduces signals to downstream kinases, phosphorylating IFN-regulatory factor3/7 (IRF3/7) (Liu et al., 2015). The phosphorylated IRF3/7 form dimers and translocate into the nucleus, initiating the induction of IFN finally.

IRF3 and IRF7 are members of the IRF family, playing vital roles in the induction of IFNs and antiviral response. They consist of several functional domains, including a conserved N-terminal DNA binding domain (DBD) responsible for binding to IFN-stimulated response elements (ISREs), an IRF-associated domain (IAD) responsible for interacting with other IRF family members, and a serine-rich domain (SRD). The activation of IRF3/7 requires phosphorylation, dimerization, and

* Corresponding author. State Key Laboratory of Developmental Biology of Freshwater Fish, College of Life Science, Hunan Normal University, Changsha, 410081, China.

** Corresponding author. State Key Laboratory of Developmental Biology of Freshwater Fish, College of Life Science, Hunan Normal University, Changsha, 410081, China.

E-mail addresses: xiaojun2018@hunnu.edu.cn (J. Xiao), fenghao@hunnu.edu.cn (H. Feng).

[1] These authors contributed equally to this paper.

https://doi.org/10.1016/j.dci.2023.104915
Received 25 June 2023; Received in revised form 3 August 2023; Accepted 13 August 2023
Available online 14 August 2023

Table 1
Primers used in the study.

Primer name	Sequence (5′-3′)	Primer information
CDS		
3nhnRNPM-F	ATGTCGACCGAGGTTAAATCA	For 3nhnRNPM CDS cloning
3nhnRNPM-R	TTATGCATTTCTGTCAATCCT	
Expression vector		
3nhnRNPM-F	ACTGACGGTACCATGTCGACCGAGGTTAAA	For expression vector construction
3nhnRNPM-R	ACTGACCTCGAGTTATGCATTTCTGTCAAT	
qRT-PCR		
q-SVCV-*M*-F	CGACCGCGCCAGTATTGATGGATAC	
q-SVCV-*M*-R	ACAAGGCCGACCCGTCAACAGAG	
q-SVCV-*N*-F	GGGTCTTTACAGAGTGGG	
q-SVCV-*N*-R	TTTGTGAGTTGCCGTTAC	
q-SVCV-*P*-F	AACAGGTATCGACTATGGAAGAGC	
q-SVCV-*P*-R	GATTCCTCTTCCCAATTGACTGTC	
q-SVCV-*G*-F	GATGACTGGGAGTTAGATGGC	
q-SVCV-*G*-R	ATGAGGGATAATATCGGCTTG	
q-epc *IFNφ1*-F	ATGAAAACTCAAATGTGGACGTA	
q-epc *IFNφ1*-R	GATAGTTTCCACCCATTTCCTTAA	
q-epc *PKR*-F	ACCTGAAGCCTCCAAACATA	
q-epc *PKR*-R	GCATTCGCTCATCATTGTC	
q-epc *Mx1*-F	TGGAGGAACCTGCCTTAAATAC	
q-epc *Mx1*-R	GTCTTTGCTGTTGTCAGAAGATTAG	
q-epc *ISG15*-F	TGATGCAAATGAGACCGTAGAT	
q-epc *ISG15*-R	CAGTTGTCTGCCGTTGTAAATC	
q-epc *actin*-F	AAGGAGAAGCTCTGCTATGTGGCT	
q-epc *actin*-R	AAGGTGGTCTCATGGATACCGCAA	
q-3nhnRNPM-F	GTGGCGTCGGTGGGCAGTTT	
q-3nhnRNPM-R	AGGCTCGCTCGGCAGTCTCA	
q-3nIFNa-F	TTCTTGCCTTGACCTTGGAT	
q-3nIFNa-R	GCTCAGATGACTGCCGTTGC	
q-3nIFNa2-F	GATTGGAGATGCTAAGGTGGAG	
q-3nIFNa2-R	AAAGTCCTGAAGTGCCTTGTTA	
shRNA		
sh3nhnRNPM-1-F	CCGGGCAACTTCGGGACTCCTTTCACTCGAGTGAAAGGAGTCCCGAAGTTGCTTTTTG	
sh3nhnRNPM-1-R	AATTCAAAAAGCAACTTCGGGACTCCTTTCACTCGAGTGAAAGGAGTCCCGAAGTTGC	
sh3nhnRNPM-2-F	CCGGGCAGATATCCTGGAAGATAAACTCGAGTTTATCTTCCAGGATATCTGCTTTTTG	
sh3nhnRNPM-2-R	AATTCAAAAAGCAGATATCCTGGAAGATAAACTCGAGTTTATCTTCCAGGATATCTGC	
sh3nhnRNPM-3-F	CCGGGCTCAACGGACGAGAGATTGACTCGAGTCAATCTCTCGTCCGTTGAGCTTTTTG	
sh3nhnRNPM-3-R	AATTCAAAAAGCTCAACGGACGAGAGATTGACTCGAGTCAATCTCTCGTCCGTTGAGC	

nuclear translocation. Thus many molecules have been shown to regulate the innate immune response by regulating the activation of IRF3/7. For instance, in mammals, the receptor for activated C kinase 1 (RACK1) suppresses the phosphorylation of IRF3/7, thereby limiting the production of type I IFNs (Qin et al., 2021). Neuralized E3 ubiquitin-protein ligase 3 (NEURL3) promotes the activity of IRF7 by facilitating K63-linked ubiquitination (Qi et al., 2022). Tripartite motif-containing protein 28 (TRIM28) acts as a negative regulator of IRF7 by enhancing the SUMOylation of IRF7 at K444 and K446 (Liang et al., 2011). Calmodulin-like 6 (CALML6) binds to the phosphorylated IRF3 and impedes its dimerization and nuclear translocation (Wang et al., 2019). Similar to mammals, the activities of IRF3/7 in teleost fish are also regulated by a variety of molecules. For example, RNASEK enhances the phosphorylation of IRF3/7, leading to increased type I IFN production (Sun et al., 2021). Ub-activating enzyme (Uba1) and rapunzel 5 (RPZ5) mediate the K48-linked ubiquitination and subsequent degradation of IRF3 and IRF7, respectively (Chen et al., 2021; Lu et al., 2019). Protein arginine methyltransferases 6 (PRMT6) in black carp promotes lysosome degradation of IRF3 and inhibits its K63-linked ubiquitination (C. Yang et al., 2023); Black carp DExD/H-box RNA helicase 19 (DDX19) interacts with IRF3 and hampers its nuclear translocation (Liu et al., 2022). Additionally, grass carp Lysine (K) acetyltransferase 8 (KAT8) enhances the acetylation of IRF3/7, thereby influencing their affinity for ISRE response elements (Li et al., 2022). In summary, whether in mammals or fish, the regulation of IRF3/7 is a complex and multifaceted process involving various molecules.

The hnRNPs family is composed of diverse RNA-binding proteins, which are typically associated with RNA metabolism, such as mRNA trafficking, alternative splicing, and translational regulation (J. Wang et al., 2022). hnRNPM, also known as CEAR, contains three RNA-recognition motifs (RRMs) and is mainly distributed in the nucleus of mammalian cells (J. Wang et al., 2022). Recent studies have revealed the roles of hnRNPM in cancer metastasis. For instance, hnRNPM promotes breast cancer metastasis by activating the switch of alternative splicing during the epithelial-mesenchymal transition and regulating the CD44 level (Sun et al., 2017; Xu et al., 2014). Additionally, quite a few studies reported that hnRNPM was related to innate immunity. For example, in vesicular stomatitis virus (VSV) infected macrophages, hnRNPM inhibits the expression of a series of innate immune transcripts, including *Mx1*, *Gbp5*, and *Rsad2* (West et al., 2019). Besides, hnRNPM restrains the RLR/IFN signaling by impairing the binding of RIG-I and MDA5 to viral RNA, and then dampening the induction of type I IFN (Cao et al., 2019). However, the function of hnRNPM in innate immune response in teleost remains unknown.

Triploid fish (3n = 150) was produced through the hybridization between the male allotetraploid (4n = 200) and the female red crucian carp (2n = 100), which outperforms its parents in disease resistance and stress resistance (Chen et al., 2009; Liu, 2010). Our previous works have identified some pivotal components of the RLR/IFN pathway, which played a vital role in the antiviral innate immune response of triploid fish (Xiao et al., 2019, 2022). However, the regulatory mechanisms of the RLR signaling pathway in triploid fish still need to be explored.

To explore the function of hnRNPM in the antiviral activity of triploid fish, the hnRNPM homologue of triploid fish (3nhnRNPM) has been cloned and identified in this paper. The reporter assay and plaque assay showed that 3nhnRNPM significantly inhibited 3nIRF7-mediated IFN

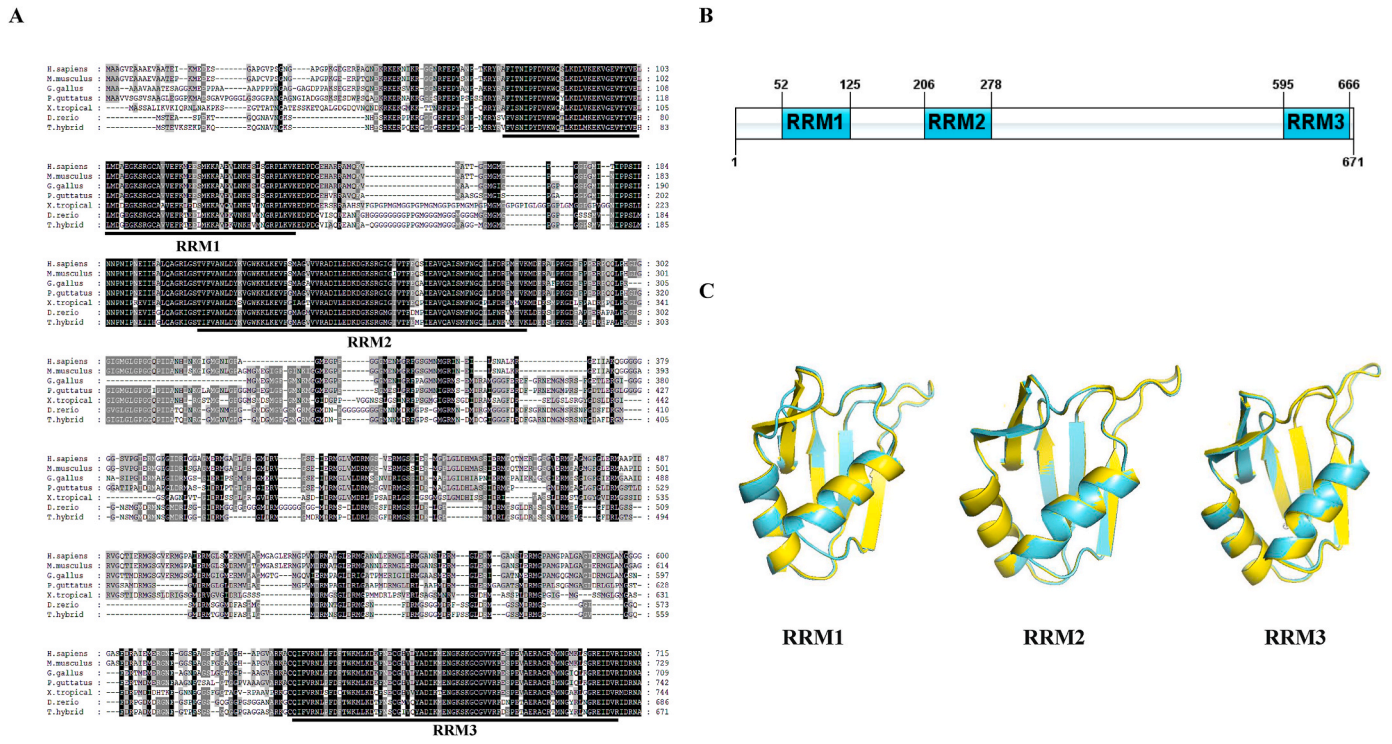

Fig. 1. Sequence and structure analysis of 3nhnRNPM
(A) Amino acid multiple sequence alignments of hnRNPM of *Homo sapiens* (XP_005272535.1), *Mus musculus* (NP_084080.1), *Gallus gallus* (NP_001026103.1), *Pantherophis guttatus* (XP_034260446.1), *Xenopus tropicalis* (XP_004911113.1), and *Danio rerio* (NP_001243560.1). (B) Schematic diagram of 3nhnRNPM protein. (C) Prediction of the spatial structure of three RNA-recognition motifs of human hnRNPM and 3nhnRNPM by α-fold2 (the images were generated in Pymol). In the pictures, the RNA-recognition motifs of human hnRNPM are color-coded with yellow, and the RNA-recognition motifs of 3nhnRNPM are color-coded with cyan. RRM: RNA-recognition motif. (For interpretation of the references to color in this figure legend, the reader is referred to the Web version of this article.)

Table 2
Comparison of vertebrate hnRNPM homologues (%).

Species	Full-length sequence		Species	Full-length sequence	
	Identity	Similarity		Identity	Similarity
Triploid hybrid	100.0	100.0	*Ovis aries*	55.6	67.9
Pimephales promelas	93.2	98.0	*Puma yagouaroundi*	55.5	67.3
Danio rerio	82.9	86.1	*Prionailurus bengalensis*	55.5	67.3
Clupea harengus	81.9	88.2	*Dromiciops gliroides*	58.0	68.8
Acanthopagrus latus	79.3	85.1	*Gracilinanus agilis*	58.0	68.8
Amphiprion ocellaris	78.5	85.5	*Panthera leo*	55.5	67.2
Perca fluviatilis	77.5	83.5	*Lonchura Striata domestica*	56.8	68.8
Betta splendens	79.3	85.4	*Rhinatrema bivittatum*	55.4	67.6
Oreochromis aureus	79.3	85.7	*Parus major*	57.2	68.8
Haplochromis burtoni	79.3	85.7	*Microcaecilia unicolor*	54.8	66.3
Polypterus senegalus	69.4	78.7	*Bubalus bubalis*	54.8	66.8
Pantherophis guttatus	61.1	71.1	*Motacilla Alba alba*	54.2	66.4
Crotalus tigris	60.1	70.2	*Homo sapiens*	54.3	65.9
Mauremys reevesii	59.4	69.1	*Corvus Cornix cornix*	54.3	66.0
Chrysemys Picta bellii	59.4	68.9	*Peromyscus Maniculatus bairdii*	55.0	66.6
Chelonia mydas	59.9	69.6	*Mesocricetus auratus*	55.0	66.6
Dermochelys coriacea	59.0	68.8	*Sus scrofa*	54.9	66.6
Zootoca vivipara	60.4	71.5	*Chlorocebus sabaeus*	54.8	66.4
Aquila Chrysaetos chrysaetos	57.3	69.0	*Jaculus jaculus*	54.5	66.4
Falco rusticolus	57.1	69.0	*Mus musculus*	54.6	66.3
Falco naumanni	57.1	69.0	*Anser cygnoides*	55.7	67.8
Panthera tigris	55.0	66.4	*Xenopus tropicalis*	55.9	67.6
Gallus gallus	54.9	66.4	*Xenopus laevis*	55.7	67.2

promoter transcription and antiviral activity. Co-immunoprecipitation assay identified an interaction between 3nhnRNPM and 3nIRF7, with a concurrent observation that 3nIRF7 was retained in the nucleus when co-expressed with 3nhnRNPM. In brief, 3nhnRNPM suppressed 3nIRF7-mediated IFN signaling in the antiviral innate immunity.

2. Materials and methods

2.1. Cells, plasmids, and transfection

HEK293T cells, HeLa cells, *Epithelioma papulosum cyprini* (EPC) cells, 2nFC (caudal fin of red crucian carp), 3nFC (caudal fin of triploid fish),

Table 3
GenBank accession numbers of vertebrate hnRNPM homologues.

Species	GenBank Accession Number	Species	GenBank Accession Number
Mammals		**Reptiles**	
Homo sapiens	XP_005272535.1	*Pantherophis guttatus*	XP_034260446.1
Mus musculus	NP_084080.1	*Crotalus tigris*	XP_039180492.1
Sus scrofa	XP_005654810.2	*Zootoca vivipara*	XP_034972775.1
Chlorocebus sabaeus	XP_037848264.1	*Mauremys reevesii*	XP_039371100.1
Ovis aries	XP_012033373.1	*Chrysemys Picta bellii*	XP_005283833.1
Bubalus bubalis	XP_025149145.1	*Dermochelys coriacea*	XP_038240423.1
Panthera tigris	XP_042833923.1	*Chelonia mydas*	XP_037741953.1
Panthera leo	XP_042784143.1	**Amphibians**	
Prionailurus bengalensis	XP_043442346.1	*Xenopus laevis*	XP_041416854.1
Puma yagouaroundi	XP_040305631.1	*Xenopus tropicalis*	XP_004911113.1
Jaculus jaculus	XP_004672260.1	*Microcaecilia unicolor*	XP_030073833.1
Mesocricetus auratus	XP_005081378.1	*Rhinatrema bivittatum*	XP_029441850.1
Peromyscus Maniculatus bairdii	XP_042123027.1	**Fishes**	
Gracilinanus agilis	XP_044528713.1	*Triploid hybrid*	OQ718809
Dromiciops gliroides	XP_043836408.1	*Danio rerio*	NP_001243560.1
Birds		*Pimephales promelas*	XP_039538131.1
Gallus gallus	NP_001026103.1	*Amphiprion ocellaris*	XP_023130250.1
Anser cygnoides	XP_013050693.1	*Haplochromis burtoni*	XP_005931018.1
Falco naumanni	XP_040448215.1	*Oreochromis aureus*	XP_031601416.1
Falco rusticolus	XP_037242160.1	*Acanthopagrus latus*	XP_036970282.1
Aquila Chrysaetos chrysaetos	XP_029889172.1	*Betta splendens*	XP_029004665.1
Motacilla Alba alba	XP_038019527.1	*Perca fluviatilis*	XP_039666486.1
Lonchura Striata domestica	XP_021401849.1	*Clupea harengus*	XP_031431023.1
Parus major	XP_015507114.1	*Polypterus senegalus*	XP_039622922.1
Corvus Cornix cornix	XP_039422119.1		

and 4nFC (caudal fin of allotetraploid) cells (Xiao et al., 2018) were kept in the lab. Mammalian cell lines were cultured in DMEM (BaseIMedia, China) containing 10% FBS, 100 U/mL penicillin, and 100 μg/mL streptomycin with 5% CO_2 at 37 °C; Fish cell lines were cultured in the same culture medium with 5% CO_2 at 26 °C.

Expression plasmids in this paper for Flag-3nMDA5a, Flag-3nMDA5b, Flag-3nMAVS, Flag-3nTBK1, Flag-3nIRF7, HA-3nhnRNPM, and Myc-3nhnRNPM were constructed into pcDNA5/FRT/TO; pRL-TK, Luci-DrIFNφ1 (zebrafish IFNφ1 promoter transcription analysis) were kept in the lab.

Cells were seeded one day before transfection and the medium was replaced with the medium containing 2% FBS before transfection. Polyethylenimine (PEI) (Yeasen, China) was used for transfection according to the manufacturer's instructions. Six hours after transfection, the cell culture medium was replaced with the medium containing 10% FBS.

2.2. Virus production, titer detection, and infection

For virus production, spring viremia of carp virus (SVCV) was propagated in EPC cells at 26 °C with 2% FBS. In brief, EPC cells in 10 cm plates were infected with SVCV. One hour later, the supernatants were removed, and the infected cells were washed with DMEM followed by incubation with DMEM containing 2% FBS. When the cytopathic effect (CPE) was up to 50%, the supernatant media and cells were harvested together. After three times of freezing and thawing, filter the virus mixture before measuring the titers.

Viral titers were determined by viral plaque assay on EPC cells as previously described (Xiao et al., 2022). Briefly, EPC cells were infected with 10-fold serially diluted viral supernatant for 1 h. The supernatant was then replaced with fresh DMEM containing 2% FBS and 0.75 percent methylcellulose. Plaques were counted on the third-day post-infection.

For cell infection, the cells were infected with SVCV at different MOIs. One hour later, the supernatants were removed and the cells were washed with DMEM followed by incubation with DMEM containing 2% FBS for 24h. For fish infection, intraperitoneal injection was used in this study. The healthy triploid hybrid fish, with an average weight of 45 ± 1.1 g, were placed in recirculating water at 26 °C and cultured for 2 weeks before experiments. Fish in the experimental group were intraperitoneally injected with SVCV (2.9×10^7 TCID50/ml). Fish in the control group were intraperitoneally injected with PBS. At 24 h post-injection, fish were dissected and tissues were collected respectively for RNA extraction and qRT-PCR analysis.

2.3. Immunoblotting (IB)

HEK293T cells or EPC cells were transfected as required and harvested after 48 h, washed once with PBS, and lysed for IB assay as previously described (X. Yang et al., 2023). Samples were boiled in 5 × SDS sample buffer for 5 min, separated on SDS-polyacrylamide gels and then transferred onto PVDF membranes (Millipore). The membranes were incubated with the indicated primary antibodies overnight at 4 °C after blocking with 5% skim milk. After three additional washes with TBST, the membranes were incubated with the corresponding secondary antibodies. BCIP/NBT Alkaline Phosphatase Color Development Kit was used to visualize protein bands (Thermo, USA).

Antibodies (Abs) used in the paper were as follows: mouse monoclonal anti-Myc Ab (Abmart, China), mouse monoclonal anti-Flag Ab (Abmart, China), mouse monoclonal anti-HA Ab (Abmart, China), mouse monoclonal anti-β-actin (Sigma, USA), rabbit monoclonal anti-LaminB1 (Abmart, China), and mouse monoclonal anti-phosphoserine Ab (Abbkine, China). The second antibodies used in this study are AP-conjugated goat anti-mouse (Sigma, USA) and AP-conjugated goat anti-rabbit (Sigma, USA).

2.4. Nucleo-cytoplasmic separation

HEK293T cells were transfected with indicated expression plasmids. At 48 h post-transfection (hpt), we harvested and lysed the cells with hypotonic buffer (0.05% NP-40, 1 mM Tris-HCl, 1.5 mM NaCl) containing protease inhibitor cocktails. Then, the samples were centrifuged at 700×*g* for 5 min and the supernatant was obtained as the cytoplasmic extract, the precipitated pellet was obtained as nuclear extract after 3 times washing.

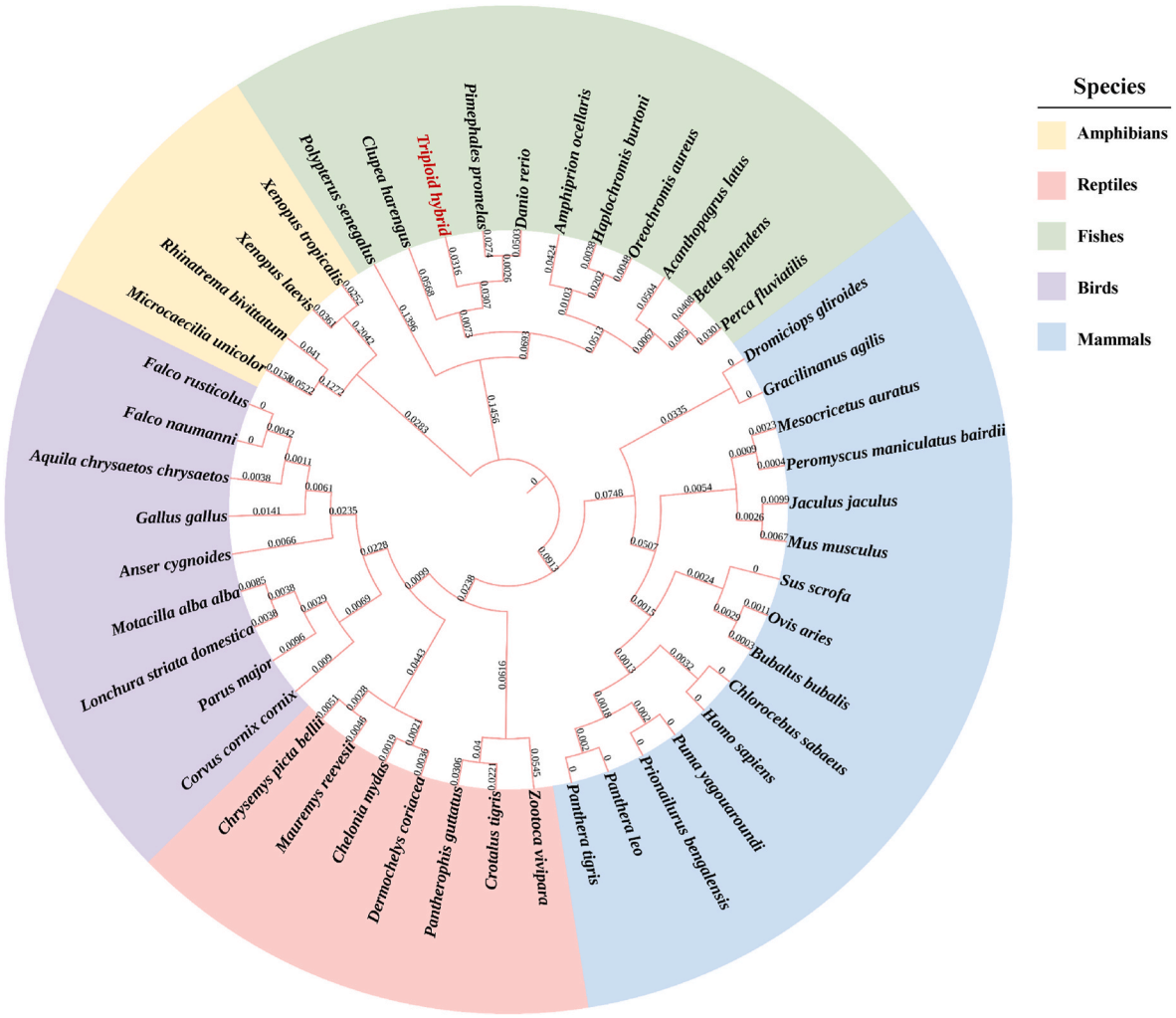

Fig. 2. Phylogenetic tree analysis of hnRNPM homologues from different vertebrates
Amino acid sequences of hnRNPM homologues were aligned (GenBank accession numbers are listed in Table 3). These species were classified into mammals, birds, reptiles, amphibians, and fishes. The result of alignment was built into a phylogenetic tree by using MEGA X through the neighbor-joining method and the phylogenetic tree was annotated by iTOL (iTOL: Interactive Tree Of Life (https://itol.embl.de/)), The numbers on the branches represent branch length.

2.5. Immunofluorescence

HeLa and 3nFC cells were transfected with HA-3nhnRNPM and fixed with 4% paraformaldehyde (Solarbio, P1110) for 15 min at 24 hpt, penetrated with 0.2% Triton X-100 for 10 min and blocked with 10% goat serum (Solarbio, SL038) subsequently. And then incubated with mouse monoclonal anti-HA Ab (1:500, Abmart) followed by incubation with Alexa Fluor 488-conjugated secondary Ab (1:1000, Invitrogen) for 1 h. Finally, the cells were washed 5 times with PBS and stained with DAPI (H1200, Vector Laboratories). The laser confocal scanning microscope (Olympus FV1200, Japan) was used to visualize and image the sample.

2.6. Immunoprecipitation (IP) and Co-immunoprecipitation (Co-IP)

HEK293T cells were co-transfected with expression plasmids as required for 48 h, harvested for IP with 1% NP40 buffer containing protease inhibitor cocktails. In brief, the cells were lysed and the supernatant was incubated with protein A/G agarose beads (Sigma, USA) and then transferred to the Flag-conjugated protein A/G agarose beads (Sigma, USA). Finally, the beads boiled in 5 × sample buffer after washing were used for IB as above.

2.7. Luciferase reporter assay

EPC cells were co-transfected with expression plasmids together with pRL-TK (25 ng), and Luci-DrIFNφ1 (250 ng). For each transfection, the total amount of plasmid DNA was balanced with the empty vector. The cells were harvested at 24 hpt and lysed by passive lysis buffer. The reporter assay was conducted based on the instruction of the manufacturer (Promega, USA).

2.8. Quantitative real-time PCR (qRT-PCR)

The relative transcription level of *SVCV-M* (*N, P, G*), epcIFNφ1, *epcISG15*, *epcPKR*, *epcMx1*, *3nhnRNPM*, *3nIFNa* and *3nIFNa2* was examined by qRT-PCR using Applied Biosystems QuantStudio 5 Real-Time PCR Systems (Thermo Fisher, USA). The program was: 1 cycle of 95 °C/10 min, 40 cycles of 95 °C/15 s, 60 °C/1 min. The data were analyzed by the $2^{-\Delta\Delta CT}$ method. The primes for qRT-PCR were listed in Table 1.

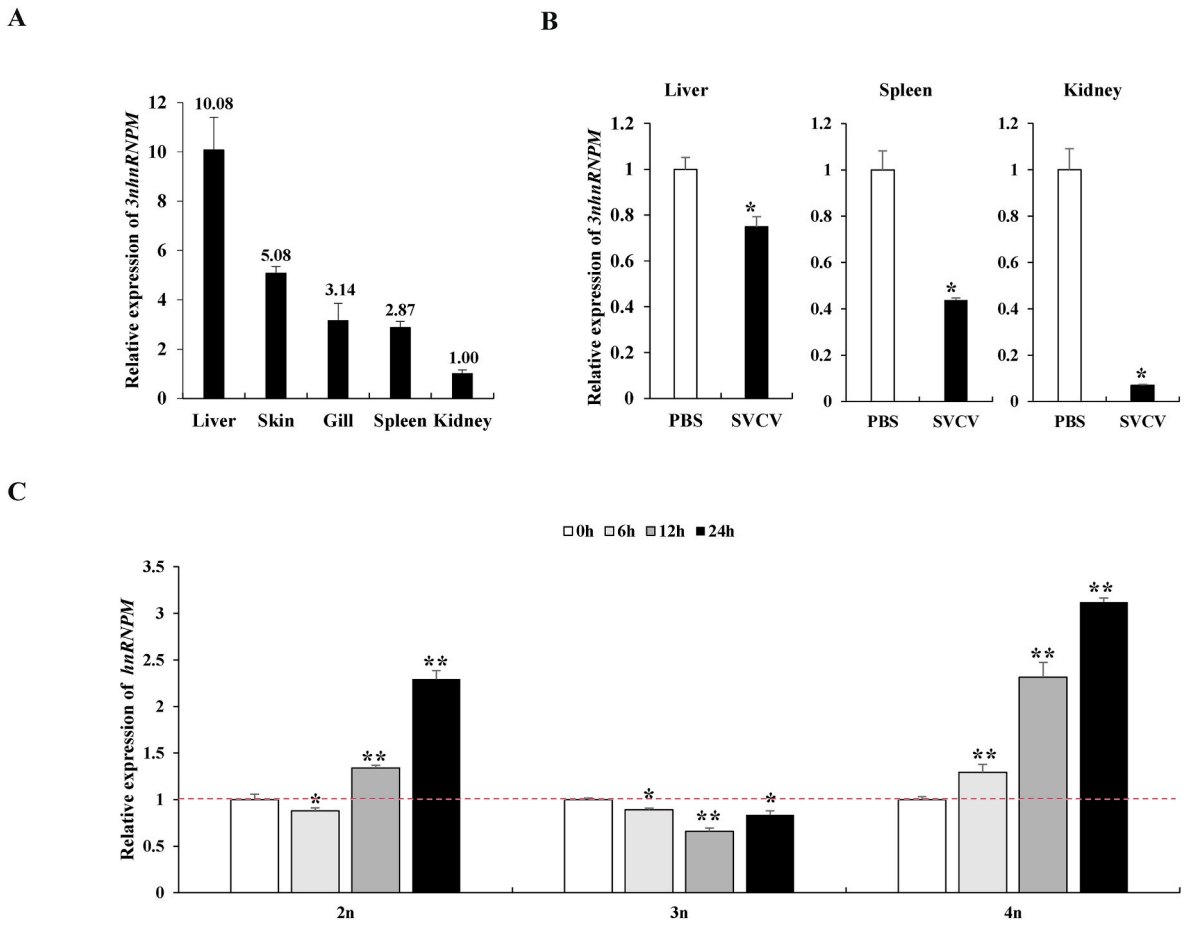

Fig. 3. 3nhnRNPM expression *in vivo* and *in vitro*
(A) The analysis of *3nhnRNPM* expression in different tissues obtained from the healthy triploid fish. The *3nhnRNPM* expression level in the kidney was used as control and set to 1. (B) The relative mRNA levels of *3nhnRNPM* in spleen, kidney, and liver at 24 h post-SVCV injection. The *3nhnRNPM* expression in the fish injected with PBS was used as the control and set to 1. (C) The relative mRNA level of *hnRNPM* homologues in 2nFC, 3nFC, and 4nFC cells at 6 h, 12 h, and 24 h after SVCV infection. The *hnRNPM* expression in the uninfected cells was used as the control and set to 1.

2.9. Gene knockdown

Several shRNA oligos (listed in Table 1) targeting 3nhnRNPM were designed through the online tool Invitrogen Block-iT RNAi Designer (thermofisher.com). Subsequently, these targeting fragments were constructed into pLKO.1-TRC cloning vector.

2.10. Statistics analysis

All assays were conducted in triplicate. The data were analyzed by two-tailed Student's t-test. Asterisk (*) stands for $p < 0.05$, and (**) stands for $p < 0.01$.

3. Results

3.1. Sequence and protein structure analysis of 3nhnRNPM

To study the role of hnRNPM in the antiviral innate immunity of triploid hybrid, 3nhnRNPM (GenBank accession number: OQ718809) has been cloned from the spleen of triploid hybrid. The coding sequence (CDS) of *3nhnRNPM* gene is composed of 2016 nucleotides, which encodes 671 amino acids (Fig. 1A and Supplemental Fig. 1). The calculated molecular mass of 3nhnRNPM is 71.4 kDa (by EXPASy).

The amino acid sequence of 3nhnRNPM was submitted to multiple alignments with that of hnRNPM from other species, containing zebrafish (*Danio rerio*), clawed frog (*Xenopus tropicalis*), snake (*Pantherophis guttatus*), house mice (*Mus musculus*), jungle fowl (*Gallus gallus*) and human (*Homo sapiens*). The comparison suggested the conservation of hnRNPM in vertebrates and the predicted 3nhnRNPM protein contains three RNA-recognition motifs at 52–125, 206–278, and 595–666 residues, respectively (Fig. 1A and B). Furthermore, the spatial structures of hnRNPM of triploid hybrid and human were built by αfold2 software, respectively (https://www. AlphaFold2.ipynb; Supplemental Fig. 2). In accordance with the amino acid sequences analysis, the spatial structures of the three RNA-recognition motifs of 3nhnRNPM show an extremely high similarity to those of human hnRNPM (Fig. 1C). To ulteriorly investigate the evolution of hnRNPM in vertebrates, the phylogenetic tree was built among the selected hnRNPM proteins which were listed in Table 2. The selected sequences of hnRNPM were clustered into 5 groups, including mammals, birds, reptiles, amphibians, and fishes. The phylogenetic analysis results showed that 3nhnRNPM was clustered with hnRNPM of fathead minnow (*Pimephales promelas*) and zebrafish (*Danio rerio*), sharing 93.2% and 82.9% sequence identity respectively (Fig. 2).

3.2. 3nhnRNPM expression in vivo and in vitro

To investigate the constitutive expressions of *3nhnRNPM* gene in different tissues, total RNA was extracted separately from the kidney, spleen, gill skin, and liver of the triploid hybrid fish for qRT-PCR. As

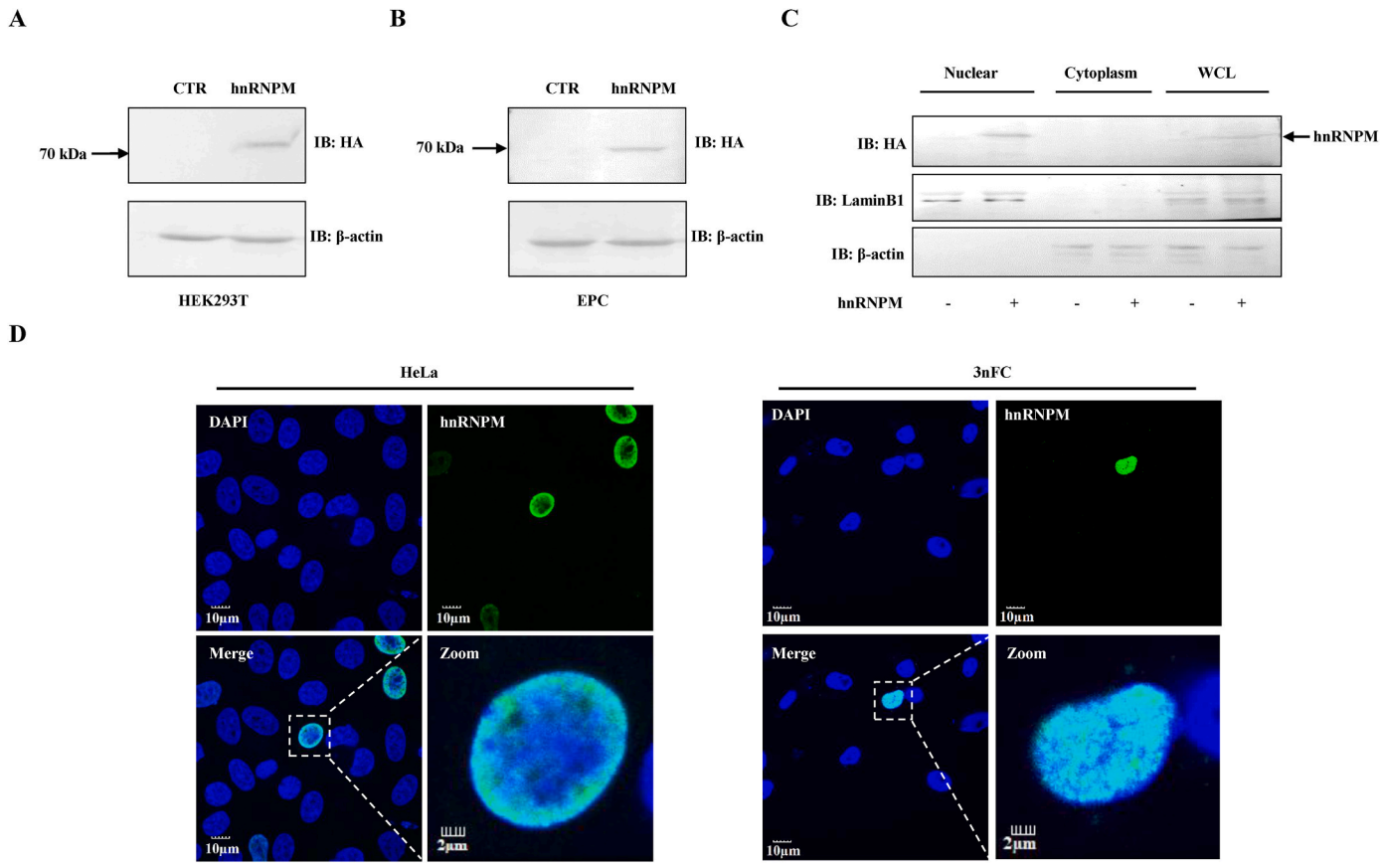

Fig. 4. Protein expression and subcellular distribution of 3nhnRNPM.
HEK293T cells (A) or EPC cells (B) in 6-well plate were transfected with HA-3nhnRNPM (3 μg) or empty vector (3 μg). Cells were harvested at 48 h post-transfection and used for immunoblotting. Control: cells transfected with the empty vector. (C) HEK293T cells in 6-well plate were transfected with HA-3nhnRNPM (3 μg) as indicated above, the transfected cells were harvested after 48 h and the cytosolic and nuclear extracts were isolated and used for immunoblot according to the methods. LaminB1 and β-actin were utilized as the nuclear and cytoplasmic internal reference, respectively. (D) HeLa cells and 3nFC cells in 24-well plate were transfected with HA-3nhnRNPM (600 ng) as indicated above and used for IF staining. The scale represents 10 μm and 2 μm, respectively.

shown in Fig. 3A, the expression level of *3nhnRNPM* was highest in the liver, followed by the skin, gill, spleen, and kidney, respectively. To clarify the expression pattern of 3nhnRNPM in response to viral infection, we examined the transcription levels of *3nhnRNPM* in immune organs, including the spleen, kidney, and liver, at 24 h post SVCV injection. The results indicated a reduction in the transcription of 3nhnRNPM in these tissues after SVCV infection (Fig. 3B). Furthermore, we studied and compared the expression patterns of *hnRNPM* in 2nFC, 3nFC, and 4nFC cells infected with SVCV over different time points. The data revealed that after SVCV infection, the transcription of *3nhnRNPM* in host cells showed a decreasing trend, whereas the transcription of its homologue in 2nFC and 4nFC showed an increasing trend (Fig. 3C). Taken together, these data suggest that 3nhnRNPM is involved in the host's antiviral immune response against SVCV infection both *in vivo* and *in vitro*.

3.3. Protein expression and subcellular distribution of 3nhnRNPM

HEK293T cells or EPC cells transfected with HA-3nhnRNPM were harvested for IB assay to investigate protein expression. As shown in Figs. 4A and 3B, the specific band of 71 kDa was detected in the whole cell lysates of both HEK293T and EPC cells expressing HA-3nhnRNPM but not in control, indicating 3nhnRNPM was well expressed in both fish and mammalian system. To further explore the subcellular localization of 3nhnRNPM, plasmids encoding HA-3nhnRNPM were overexpressed in HeLa cells and 3nFC cells for immunofluorescence staining assay. The results demonstrated that 3nhnRNPM (green fluorescent signals) was concentrated in the nucleus (Fig. 4D). Meanwhile, HEK293T cells transfected with HA-3nhnRNPM were harvested at 48 hpt for nucleo-cytoplasmic separation. As shown in Fig. 4C, the bands representing β-actin were only detected in cytoplasmic protein and whole cell lysates, while the bands representing laminB1 were only detected in nuclear protein and whole cell lysates, which demonstrated that the nucleus and cytoplasm were completely separated. And the specific bands of 3nhnRNPM were only detected in nuclear protein but not in cytoplasmic protein. These results demonstrated that 3nhnRNPM was substantially localized in the nucleus.

3.4. RLR/IFN signaling regulated by 3nhnRNPM

The RLR/IFN signaling pathway is crucial for the induction of IFN and antiviral innate immune responses in triploid hybrid. To investigate the effects of 3nhnRNPM on the RLR/IFN signaling, EPC cells were transfected with 3nhnRNPM for luciferase reporter assay. The data demonstrated that transfection with 3nhnRNPM alone, at varying doses, had no discernible effect on the transcription of the DrIFNφ1 promoter (Fig. 5A). However, when 3nhnRNPM was co-transfected with the crucial molecules in the RLR/IFN pathway in triploid fish, such as 3nMDA5a, 3nMDA5b, 3nMAVS, 3nTBK1 and 3nIRF7, 3nhnRNPM drastically reduced the activation on DrIFNφ1 promoter mediated by these factors (Fig. 5B ~ F). Thus, the data proved that 3nhnRNPM played a negative role in RLR/IFN cascade and implied that 3nhnRNPM functioned on 3nIRF7 in this cascade.

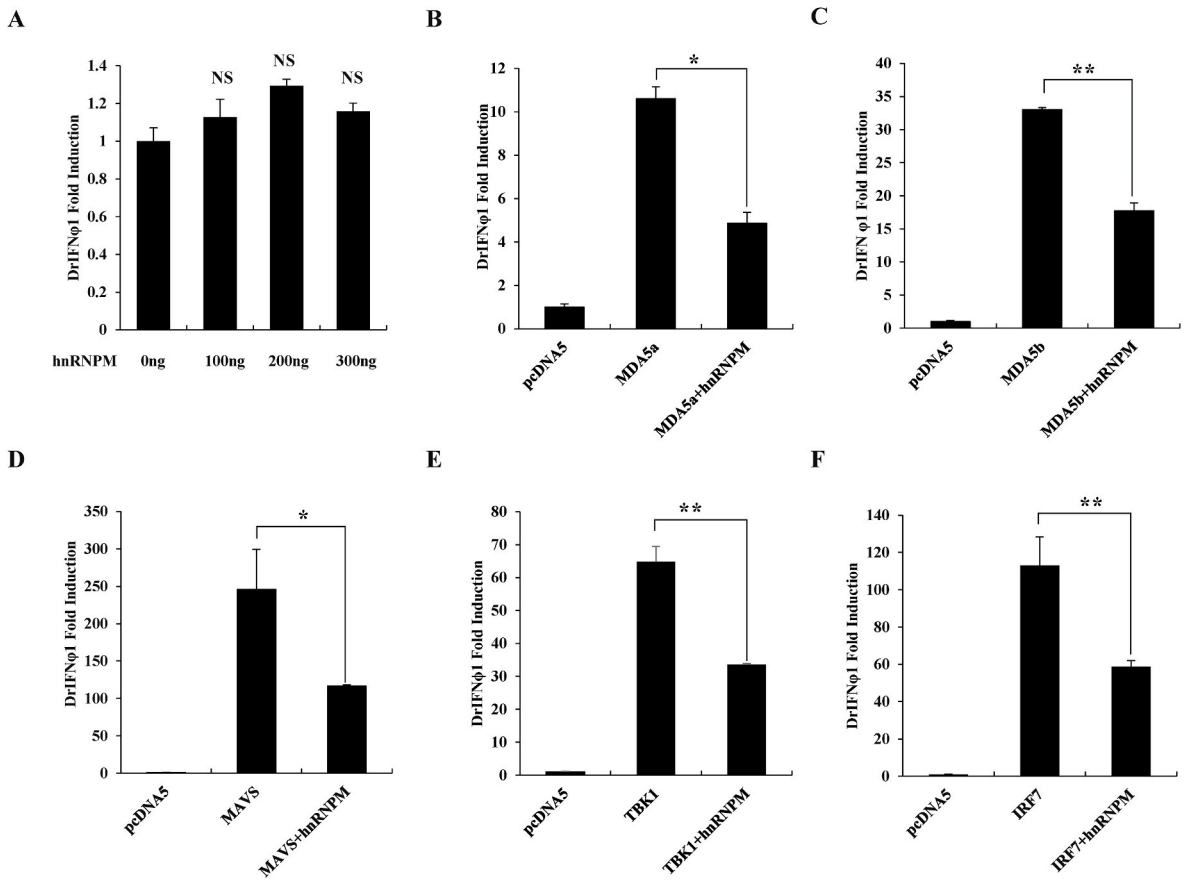

Fig. 5. RLR/IFN signaling regulated by 3nhnRNPM

EPC cells in 24-well plate were transfected with the indicated plasmids, respectively and applied to reporter assay. For each transfection, the total amount of DNA (675 ng) was balanced with the empty vector. The numbers above the error bars stand for the average IFN fold induction. hnRNPM: pcDNA5/FRT/TO-HA-3nhnRNPM MDA5a: pcDNA5/FRT/TO-Flag-3nMDA5a, MDA5b: pcDNA5/FRT/TO-Flag-3nMDA5b, MAVS: pcDNA5/FRT/TO-Flag-3nMAVS, TBK1: pcDNA5/FRT/TO-Flag-3nTBK1, IRF7: pcDNA5/FRT/TO-Flag-3nIRF7. pcDNA5: pcDNA5/FRT/TO empty vectors. Data are representative of three independent experiments.

3.5. 3nhnRNPM suppressed 3nIRF7-mediated antiviral activity

Investigations in mammals and teleost fish have determined IRF7 as a key transcription activator in IFN production during the antiviral innate immune response. For examining the impact of 3nhnRNPM on 3nIRF7-mediated antiviral activity, EPC cells were co-transfected with 3nIRF7 and/or 3nhnRNPM and exposed to SVCV infection using various MOIs (0.1/0.01/0.001). At 24 h post-infection (hpi), the media was used for the titration of SVCV, and the cells were harvested for RNA extraction and subsequential qRT-PCR. As depicted in Fig. 6A, EPC cells transfected with 3nIRF7 displayed significantly improved antiviral activity against SVCV compared with the control and the EPC cells transfected with 3nhnRNPM exhibited antiviral activity comparable to the control. However, the SVCV titer of the cells expressing both 3nIRF7 and 3nhnRNPM was much higher than that of the cells expressing 3nIRF7 alone, which proves that 3nhnRNPM obviously suppressed the 3nIRF7-mediated antiviral activity against SVCV (Fig. 6A). Furthermore, qRT-PCR assays were used to examine the replication of SVCV, revealing that the viral mRNA copies of SVCV (*M, N, P* and *G genes*) in cells expressing 3nIRF7 and 3nhnRNPM were considerably higher than those in cells expressing 3nIRF7 alone (Fig. 6B ~ E). Concurrently, the transcription levels of *epcIFNφ1* and three typical IFN-stimulated genes (*epcISG15*, *epcPKR*, and *epcMx1*) were examined separately. The data showed that the mRNA levels of *epcIFNφ1* (Fig. 7A), *epcISG15* (Fig. 7B), *epcPKR* (Fig. 7C), and *epcMx1* (Fig. 7D) induced by 3nIRF7 were dramatically suppressed by 3nhnRNPM. Collectively, these findings confirm that 3nhnRNPM impaired 3nIRF7-mediated antiviral activity in EPC cells.

3.6. Knockdown of 3nhnRNPM promoted the antiviral activity of host cells

To investigate the impact of 3nhnRNPM on host antiviral activity, shRNAs targeting this gene were designed and the knockdown efficiency was tested via western blot. Specifically, sh3nhnRNPM-2 markedly decreased the protein expression level of 3nhnRNPM (Fig. 8A). Besides, sh3nhnRNPM-2 also suppressed the transcriptional levels of endogenous hnRNPM (Fig. 8B). Subsequently, 3nFC cells transfected with sh3nhnRNPM-2 or scramble were infected with SVCV. The medium was collected for SVCV titration, and the cells were harvested for RNA extraction and subsequential qRT-PCR. Notably, the SVCV titer in the medium of 3nFC cells that transfected with shhnRNPM was significantly decreased compared to the control (Fig. 8D). Additionally, the transcriptional levels of the *M, N, P,* and *G* genes of SVCV were dramatically decreased in the 3nFC cells which transfected with shhnRNPM (Fig. 8E). On the other hand, the transcriptional levels of the *3nIFNa* and *3nIFNa2* were significantly increased in 3nhnRNPM silenced cells (Fig. 8C). To summarize, the above data demonstrated that knockdown of 3nhnRNPM promotes host cell's antiviral activity.

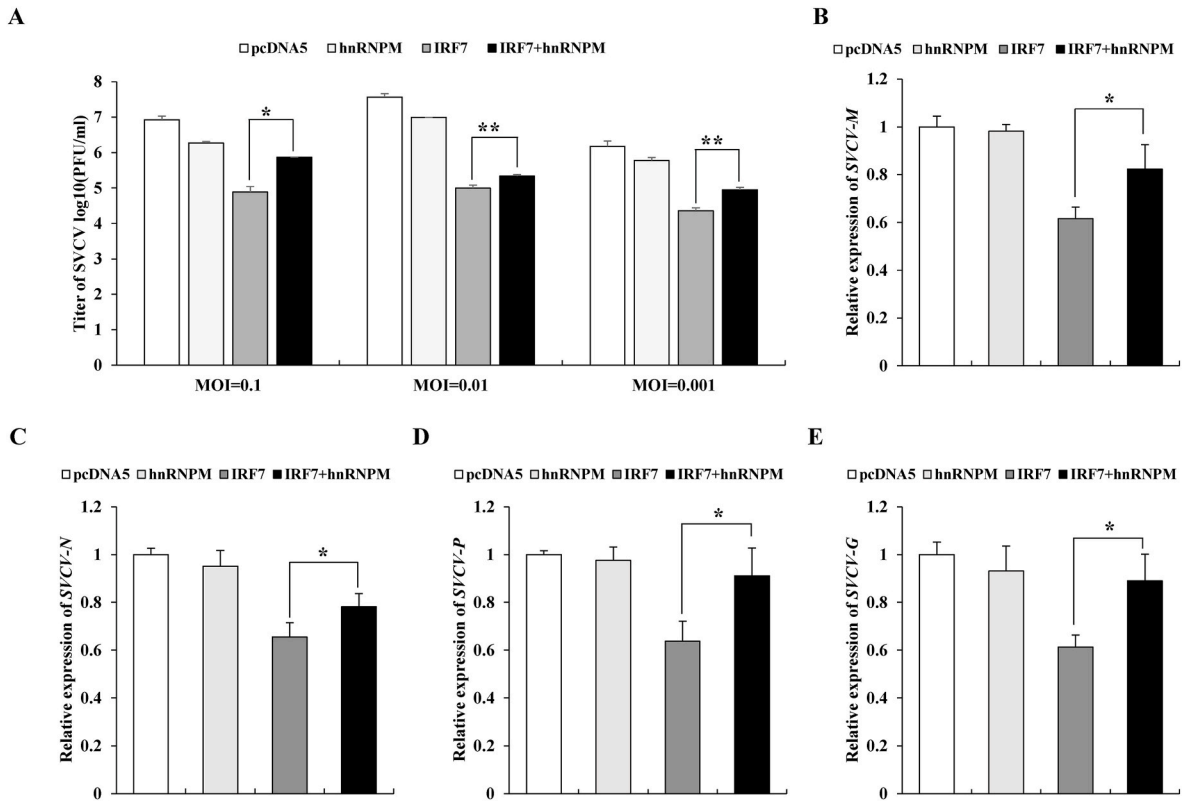

Fig. 6. 3nhnRNPM suppressed 3nIRF7-mediated antiviral activity
EPC cells in 24-well plate were co-transfected 3nhnRNPM (300 ng) and/or 3nIRF7 (300 ng) respectively, which were infected with SVCV at indicated MOI at 24 hpt. (A) The supernatants of the cells were used for virus titration. (B–E) The cells infected with SVCV at MOI = 0.01 were harvested and used for RNA isolation and subsequential qRT-PCR at 24 hpi as described in the methods. hnRNPM: pcDNA5/FRT/TO-HA-3nhnRNPM; Flag-3nIRF7: pcDNA5/FRT/TO-Flag-3nIRF7.

3.7. 3nhnRNPM interacted with and enhanced the nuclear detaining of 3nIRF7

To ulteriorly investigated the relationship between 3nhnRNPM and 3nIRF7, we conducted co-IP assays in HEK293T cells. As shown in Fig. 9A, a specific band of Myc-3nhnRNPM was detected in Flag-3nIRF7 precipitated proteins, indicating the association between 3nhnRNPM and 3nIRF7.

Phosphorylation is a key event for IRF7 activation because the molecule needs to be phosphorylated before it translocated to the nucleus and activated interferon transcription. Therefore, we examined whether 3nhnRNPM could impact the phosphorylation and nuclear migration of 3nIRF7. We transfected HEK293T cells with 3nIRF7 and/or 3nhnRNPM and performed immunoprecipitation to determine the phosphorylation levels of 3nIRF7. The results demonstrate that 3nhnRNPM did not affect the phosphorylation level of 3nIRF7 (Fig. 9B).

Next, we used a nucleo-cytoplasmic separation assay to measure the nuclear migration of 3nIRF7. Our results revealed that 3nhnRNPM improved the protein level of 3nIRF7, and also obviously enhanced the proportion of 3nIRF7 in the nucleus. Specifically, the proportion of nuclear 3nIRF7 was 49% when overexpressed alone, while the proportion increased to 79% when it co-expressed with 3nhnRNPM (Fig. 9C). Thus, our data suggested that 3nhnRNPM interacted with 3nIRF7 in the nucleus, which led to the increased nuclear detaining and delayed cytosolic degradation of 3nIRF7.

4. Discussion

The precise regulation of the RLR signaling pathway is crucial for the production of IFN and promoting immune responses against viral infection. Different host molecules, such as ubiquitin ligases/deubiquitinases, posttranslational modifiers, protein kinases/phosphatases, RNA-binding proteins, or other host proteins, cooperate to control the signal transduction of the RLR signaling (Onomoto et al., 2021). Previous studies in mammals have revealed that hnRNPM is an inhibitor of the RLR signaling pathway targeting RIG-I and MDA5. In the current study, we identified 3nhnRNPM as a negative regulator of 3nIRF7.

Sequence analysis of 3nhnRNPM demonstrated that the sequences of three RRM domains in 3nhnRNPM were highly similar to those of other vertebrates, including mammals, birds, reptiles, amphibians, and fishes (Fig. 1A), which implied the function of hnRNPM in vertebrates may be conservative. Consistent with this speculation, overexpression of 3nhnRNPM significantly suppressed the activation of DrIFNφ1 promoter mediated by 3nMDA5, 3nMAVS, 3nTBK1, and 3nIRF7 (Fig. 5). Conversely, the knockdown of 3nhnRNPM significantly enhanced the transcription of IFN and promoted the antiviral activity of host cells (Fig. 8). Furthermore, we confirmed that 3nhnRNPM interacted with 3nIRF7, and found that 3nhnRNPM increased the nuclear detaining of 3nIRF7 but showed no effect on the phosphorylation of 3nIRF7 (Fig. 9). These data established a negative regulatory function of 3nhnRNPM target 3nIRF7, but the specific mechanism remains to be elucidated. According to a previous study, human IRF7 was hijacked by IFI204 in the nucleus, thereby hindering the binding of IRF7 to the downstream ISRE. Thus, further exploration is needed to determine whether

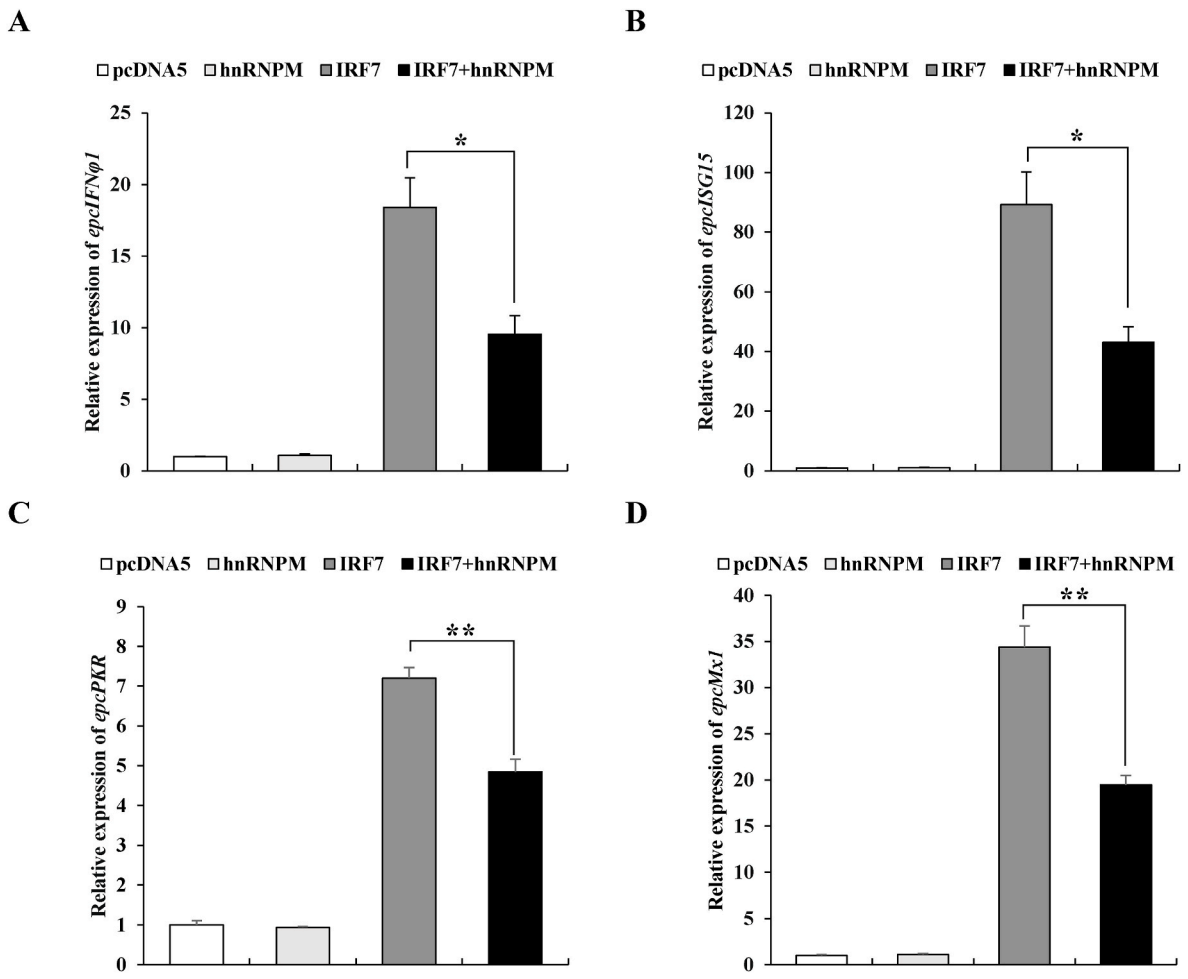

Fig. 7. 3nhnRNPM suppressed 3nIRF7-induced transcription levels of IFN-related genes
(A D) EPC cells in 24-well plate were co-transfected 3nhnRNPM (300 ng) and/or 3nIRF7 (300 ng) respectively, which were infected with SVCV (MOI = 0.01) at 24 hpt. The cells were harvested at 24 hpi and used for RNA isolation and subsequential qRT-PCR. The mRNA levels of *epcIFNφ1* (A), *epcISG15* (B), *epcPKR* (C) and *epcMx1* (D) were detected respectively. hnRNPM: pcDNA5/FRT/TO-HA-3nhnRNPM; Flag-3nIRF7: pcDNA5/FRT/TO-Flag-3nIRF7.

3nhnRNPM inhibits 3nIRF7 through a similar mechanism. It is interesting that the transcription of hnRNPM homologue in 2nFC, 3nFC, and 4nFC showed different trends in response to SVCV infection: it showed a decreasing trend in 3nFC while an increasing trend in 2nFC and 4nFC (Fig. 3C). Our previous results showed that the antiviral capacity against SVCV of 3nFC was significantly stronger than that of 2nFC and 4nFC. In addition, in response to SVCV infection, the expression of the antiviral factors such as IFN, PKR, and Mx1 in 3nFC was significantly quicker and higher than that of their expression in 2nFC and 4nFC (Xiao et al., 2018). Therefore, we hypothesized that differential expression of some negative regulators, such as hnRNPM, may be one of the potential factors leading to a faster immune response in 3nFC than in 2nFC and 4nFC.

On the other hand, members of the hnRNP family are reported to involve in several steps of the viral infection process and could associate with the protein of viruses (J. Wang et al., 2022). For instance, hnRNPA1 has been shown to interact with the N protein of porcine epidemic diarrhea virus (PEDV), thereby promoting viral replication (Li et al., 2018). And the hnRNP C was reported to associate with the N protein of IAV and implicated its replication (Tang et al., 2022); hnRNP K was reported to inhibit the replication of PEDV by degrading the N Protein of PEDV(Qin et al., 2022). However, there is no research on the relationship between hnRNPM and viral proteins. Spring viremia of carp virus (SVCV) encodes five structural proteins: phosphoprotein P, nucleoprotein N, glycoprotein G, matrix protein M, and RNA-dependent RNA polymerase L (Ashraf et al., 2016). Several studies have revealed that SVCV employs strategies to evade the host's innate immune response by targeting the IFN signaling pathway. For instance, SVCV N protein was reported to degrade MAVS and STING through the ubiquitin-proteasome pathway and autophagy-lysosome pathway respectively (Lu et al., 2016; Wang et al., 2023). SVCV P protein could interact with TBK1 and competed with IRF3 for phosphorylation which was activated by TBK1, leading to the reduction of IRF3 phosphorylation and IFN transcription (Li et al., 2016). Additionally, SVCV M protein was reported to impair IFN responses by competitively recruiting TRAF3 from the MAVS platform and suppress TRAF3 activation by inhibiting K63-linked polyubiquitination (Y.-Y. Wang et al., 2022). Therefore, it would be worthwhile to investigate if hnRNPM interacts with SVCV-encoded proteins and assists the viral infection in our future study.

In conclusion, our study suggests that 3nhnRNPM is a negative regulator of 3nIRF7, which limits the antiviral activity of 3nIRF7 by increasing its nuclear retention. Our findings will contribute to a better understanding of the regulatory mechanisms of IFN signaling in teleost.

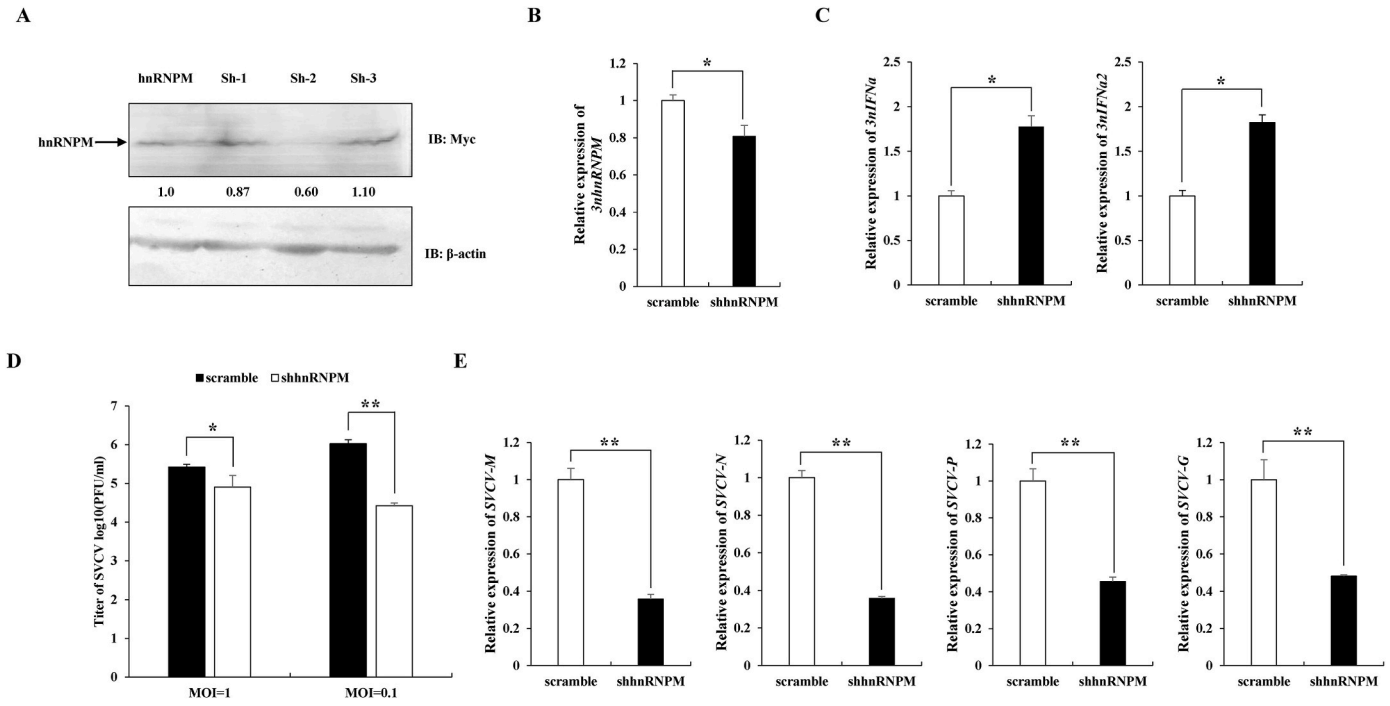

Fig. 8. Knockdown of 3nhnRNPM promoted host antiviral activity
(A) HEK293T cells were co-transfected with Myc-3nhnRNPM (1.5 μg) and scramble (or sh3nhnRNPM-1, -2, and -3) (1.5 μg), respectively. Cells were harvested at 48 hpt and used for immunoblotting. (B&C) 3nFC cells 6-well plates were transfected with sh3nhnRNPM-2 (3 μg) or scramble (3 μg), and the mRNA levels of endogenous *hnRNPM, IFNa and IFNa2* were detected by qRT-PCR, respectively. (C ~ E) 3nFC cells transfected with sh3nhnRNPM-2 or scramble were subjected to SVCV infection at 24 hpt with MOI = 1, or 0.1, and the media was used for the titration of SVCV at 24 hpi (D). Besides, the cells infected with SVCV at the MOI of 0.1 were harvested for RNA extraction isolation and subsequential qRT-PCR (C&E).

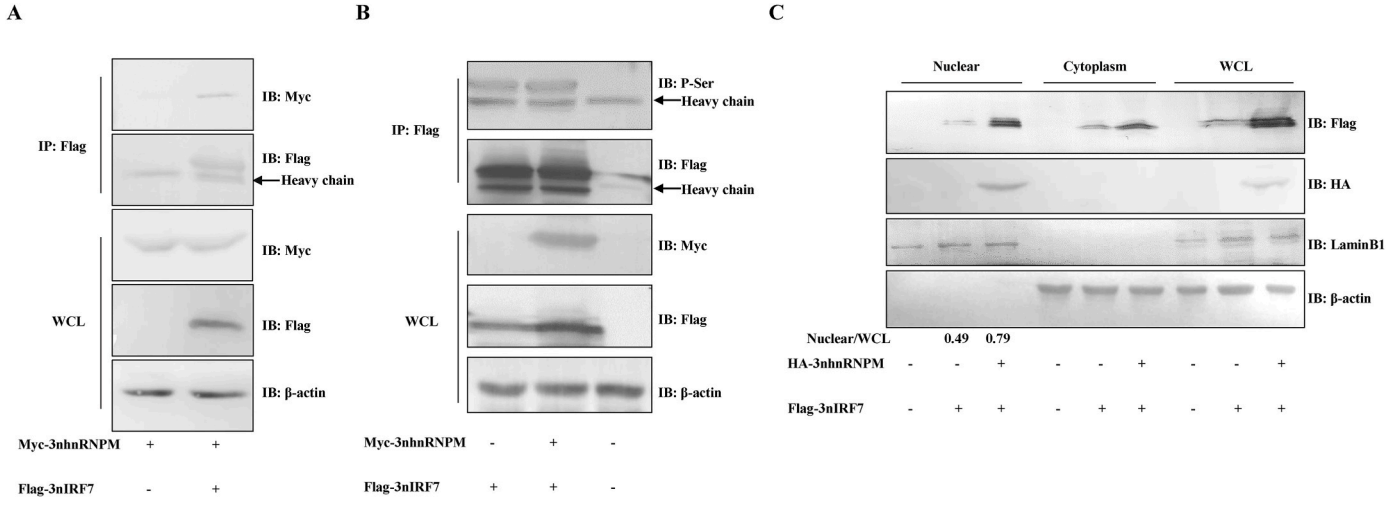

Fig. 9. 3nhnRNPM interacted with and enhanced nuclear detaining of 3nIRF7
(A&B) HEK293T cells were co-transfected with Myc-3nhnRNPM (7.5 μg) and/or Flag-3nIRF7 (7.5 μg), and the expression of 3nIRF7 was detected using the antibodies shown in the figures. (C) HEK293T cells seeded in 6-well plate were transfected with 3nIRF7 (1.5 μg) with or without 3nhnRNPM (1.5 μg) and harvested at 48 hpt. The cytosolic and nuclear extracts were isolated subsequently and used for immunoblot according to the methods. LaminB1 and β-actin were utilized as the nuclear and cytoplasmic internal reference, respectively. IB: immunoblot; IP: immunoprecipitation; WCL: whole cell lysate; Myc-3nhnRNPM: pcDNA5/FRT/TO-Myc-3nhnRNPM; Flag-3nIRF7: pcDNA5/FRT/TO-Flag-3nIRF7.

Data availability

Data will be made available on request.

Acknowledgements

This work was supported by the National Natural Science Foundation of China (31920103016, U21A20268, 32002383), Hunan Provincial Science and Technology Department (2021NK2025, 2023JJ40435), the Modern Agricultural Industry Program of Hunan Province, the Research and Development Platform of Fish Disease and Vaccine for Post-graduates in Hunan Province, College Students Research Learning and Innovative Experiment Project of Hunan Normal University (2023064, 2023063, 2023060).

Appendix A. Supplementary data

Supplementary data to this article can be found online at https://doi.org/10.1016/j.dci.2023.104915.

References

Ashraf, U., Lu, Y., Lin, L., Yuan, J., Wang, M., Liu, X., 2016. Spring viraemia of carp virus: recent advances. J. Gen. Virol. 97, 1037–1051. https://doi.org/10.1099/jgv.0.000436.

Cao, P., Luo, W.-W., Li, C., Tong, Z., Zheng, Z.-Q., Zhou, L., Xiong, Y., Li, S., 2019. The heterogeneous nuclear ribonucleoprotein hnRNPM inhibits RNA virus-triggered innate immunity by antagonizing RNA sensing of RIG-I-like receptors. PLoS Pathog. 15, e1007983 https://doi.org/10.1371/journal.ppat.1007983.

Chen, D.-D., Jiang, J.-Y., Lu, L.-F., Zhang, C., Zhou, X.-Y., Li, Z.-C., Zhou, Y., Li, S., 2021. Zebrafish Uba1 degrades IRF3 through K48-linked ubiquitination to inhibit IFN production. J. Immunol. 207, 512–522. https://doi.org/10.4049/jimmunol.2100125.

Chen, S., Wang, J., Liu, S., Qin, Q., Xiao, J., Duan, W., Luo, K., Liu, J., Liu, Y., 2009. Biological characteristics of an improved triploid crucian carp. Sci. China, Ser. A C 52, 733–738. https://doi.org/10.1007/s11427-009-0079-3.

Chen, S.N., Zou, P.F., Nie, P., 2017. Retinoic acid-inducible gene I (RIG-I)-like receptors (RLRs) in fish: current 478 knowledge and future perspectives. Immunology 151, 16–25. https://doi.org/10.1111/imm.12714.

Li, M., Hu, J., Mao, H., Li, D., Jiang, Z., Sun, Z., Yu, T., Hu, C., Xu, X., 2022. Grass carp (Ctenopharyngodon idella) KAT8 inhibits IFN 1 response through acetylating IRF3/IRF7. Front. Immunol. 12, 808159 https://doi.org/10.3389/fimmu.2021.808159.

Li, S., Lu, L.-F., Wang, Z.-X., Lu, X.-B., Chen, D.-D., Nie, P., Zhang, Y.-A., 2016. The P protein of spring viremia of carp virus negatively regulates the fish interferon response by inhibiting the kinase activity of TANK-binding kinase 1. J. Virol. 90, 10728–10737. https://doi.org/10.1128/JVI.01381-16.

Li, Z., Zeng, W., Ye, S., Lv, J., Nie, A., Zhang, B., Sun, Y., Han, H., He, Q., 2018. Cellular hnRNP A1 interacts with nucleocapsid protein of porcine epidemic diarrhea virus and impairs viral replication. Viruses 10, 127. https://doi.org/10.3390/v10030127.

Liang, Q., Deng, H., Li, X., Wu, X., Tang, Q., Chang, T.-H., Peng, H., Rauscher, F.J., Ozato, K., Zhu, F., 2011. Tripartite motif-containing protein 28 is a small ubiquitin-related modifier E3 ligase and negative regulator of IFN regulatory factor 7. J. Immunol. 187, 4754–4763. https://doi.org/10.4049/jimmunol.1101704.

Liu, S., 2010. Distant hybridization leads to different ploidy fishes. Sci. China Life Sci. 53, 416–425. https://doi.org/10.1007/s11427-010-0057-9.

Liu, S., Cai, X., Wu, J., Cong, Q., Chen, X., Li, T., Du, F., Ren, J., Wu, Y.-T., Grishin, N.V., Chen, Z.J., 2015. Phosphorylation of innate immune adaptor proteins MAVS, STING, and TRIF induces IRF3 activation. Science 347, aaa2630. https://doi.org/10.1126/science.aaa2630.

Liu, Y., Xiao, J., Qiao, G., Wang, Q., Yang, X., Xu, X., Li, J., Zhang, J., Chang, M., Feng, H., 2022. DDX19 inhibits RLR/IRF3 mediated type I interferon signaling of black carp Mylopharyngodon piceus by restricting IRF3 from entering nucleus. Aquaculture 553, 738087. https://doi.org/10.1016/j.aquaculture.2022.738087.

Lu, L.-F., Li, S., Lu, X.-B., LaPatra, S.E., Zhang, N., Zhang, X.-J., Chen, D.-D., Nie, P., Zhang, Y.-A., 2016. Spring viremia of carp virus N protein suppresses fish IFNφ1 production by targeting the mitochondrial antiviral signaling protein. J. Immunol. 196, 3744–3753. https://doi.org/10.4049/jimmunol.1502038.

Lu, L.-F., Zhou, X.-Y., Zhang, C., Li, Z.-C., Chen, D.-D., Liu, S.-B., Li, S., 2019. Zebrafish RPZ5 degrades phosphorylated IRF7 to repress interferon production. J. Virol. 93, e01272-19 https://doi.org/10.1128/JVI.01272-19.

Onomoto, K., Onoguchi, K., Yoneyama, M., 2021. Regulation of RIG-I-like receptor-mediated signaling: interaction between host and viral factors. Cell. Mol. Immunol. 18, 539–555. https://doi.org/10.1038/s41423-020-00602-7.

Qi, F., Zhang, X., Wang, L., Ren, C., Zhao, X., Luo, J., Lu, D., 2022. E3 ubiquitin ligase NEURL3 promotes innate antiviral response through catalyzing K63-linked ubiquitination of IRF7. Faseb. J. 36, e22409 https://doi.org/10.1096/fj.202200316R.

Qin, C., Niu, C., Shen, Z., Zhang, Y., Liu, G., Hou, C., Dong, J., Zhao, M., Cheng, Q., Yang, X., Zhang, J., 2021. RACK1 T50 phosphorylation by AMPK potentiates its binding with IRF3/7 and inhibition of type 1 IFN production. J. Immunol. 207, 1411–1418. https://doi.org/10.4049/jimmunol.2100086.

Qin, W., Kong, N., Wang, C., Dong, S., Zhai, H., Zhai, X., Yang, X., Ye, C., Ye, M., Tong, W., Liu, C., Yu, L., Zheng, H., Yu, H., Lan, D., Zhang, W., Tong, G., Shan, T., 2022. hnRNP K degrades viral nucleocapsid protein and induces type I IFN production to inhibit porcine epidemic diarrhea virus replication. J. Virol. 96, e0155522 https://doi.org/10.1128/jvi.01555-22.

Rehwinkel, J., Gack, M.U., 2020. RIG-I-like receptors: their regulation and roles in RNA sensing. Nat. Rev. Immunol. 20, 537–551. https://doi.org/10.1038/s41577-020-0288-3.

Sun, H., Liu, T., Zhu, D., Dong, X., Liu, F., Liang, X., Chen, C., Shao, B., Wang, M., Wang, Y., 2017. HnRNPM and CD44s expression affects tumor aggressiveness and predicts poor prognosis in breast cancer with axillary lymph node metastases: HNRNPM, CD44S, and Breast Cancer with Axillary LNM. Genes Chromosomes Cancer 56, 598–607. https://doi.org/10.1002/gcc.22463.

Sun, Z.-C., Jiang, Z., Xu, X., Li, M., Zeng, Q., Zhu, Y., Wang, S., Li, Y., Tian, X.-L., Hu, C., 2021. Fish paralog proteins RNASEK-a and -b enhance type I interferon secretion and promote apoptosis. Front. Immunol. 12, 762162 https://doi.org/10.3389/fimmu.2021.762162.

Tang, Y.-S., So, W.-K., Ng, K.-L.A., Mok, K.-P.C., Shaw, P.-C., 2022. Interaction of influenza A nucleoprotein with host hnRNP-C is implicated in viral replication. Int. J. Mol. Sci. 23, 13613 https://doi.org/10.3390/ijms232113613.

Wang, J., Sun, D., Wang, M., Cheng, A., Zhu, Y., Mao, S., Ou, X., Zhao, X., Huang, J., Gao, Q., Zhang, S., Yang, Q., Wu, Y., Zhu, D., Jia, R., Chen, S., Liu, M., 2022. Multiple functions of heterogeneous nuclear ribonucleoproteins in the positive single-stranded RNA virus life cycle. Front. Immunol. 13, 989298 https://doi.org/10.3389/fimmu.2022.989298.

Wang, X.-L., Li, Z.-C., Zhang, C., Jiang, J.-Y., Han, K.-J., Tong, J.-F., Yang, X.-L., Chen, D.-D., Lu, L.-F., Li, S., 2023. Spring viremia of carp virus N protein negatively regulates IFN induction through autophagy-lysosome-dependent degradation of STING. J. Immunol. 210, 72–81. https://doi.org/10.4049/jimmunol.2200477.

Wang, Y.-Y., Chen, Y.-L., Ji, J.-F., Fan, D.-D., Lin, A.-F., Xiang, L.-X., Shao, J.-Z., 2022. Negative regulatory role of the spring viremia of carp virus matrix protein in the host interferon response by targeting the MAVS/TRAF3 signaling Axis. J. Virol. 96, e0079122 https://doi.org/10.1128/jvi.00791-22.

Wang, Z., Sheng, C., Yao, C., Chen, H., Wang, D., Chen, S., 2019. The EF-hand protein CALML6 suppresses antiviral innate immunity by impairing IRF3 dimerization. Cell Rep. 26, 1273–1285.e5. https://doi.org/10.1016/j.celrep.2019.01.030.

West, K.O., Scott, H.M., Torres-Odio, S., West, A.P., Patrick, K.L., Watson, R.O., 2019. The splicing factor hnRNP M is a critical regulator of innate immune gene expression in macrophages. Cell Rep. 29, 1594–1609.e5. https://doi.org/10.1016/j.celrep.2019.09.078.

Xiao, J., Fu, Y., Wu, H., Chen, X., Liu, S., Feng, H., 2019. MAVS of triploid hybrid of red crucian carp and allotetraploid possesses the improved antiviral activity compared with the counterparts of its parents. Fish Shellfish Immunol. 89, 18–26. https://doi.org/10.1016/j.fsi.2019.03.044.

Xiao, J., Fu, Y., Zhou, W., Peng, L., Xiao, J., Liu, S., Feng, H., 2018. Establishment of fin cell lines and their use to study the immune gene expression in cyprinid fishes with different ploidy in rhabdovirus infection. Dev. Comp. Immunol. 88, 55–64. https://doi.org/10.1016/j.dci.2018.07.007.

Xiao, J., Zhong, H., Yan, J., Li, Z., Liu, S., Feng, H., 2022. Identification and comparative study of melanoma differentiation-associated gene 5 homologues of triploid hybrid fish and its parents. Dev. Comp. Immunol. 127, 104294 https://doi.org/10.1016/j.dci.2021.104294.

Xu, Y., Gao, X.D., Lee, J.-H., Huang, H., Tan, H., Ahn, J., Reinke, L.M., Peter, M.E., Feng, Y., Gius, D., Siziopikou, K.P., Peng, J., Xiao, X., Cheng, C., 2014. Cell type-restricted activity of hnRNPM promotes breast cancer metastasis via regulating alternative splicing. Genes Dev. 28, 1191–1203. https://doi.org/10.1101/gad.241968.114.

Yang, C., Yang, S., Miao, Y., Shu, J., Peng, Y., Li, J., Wu, H., Zou, J., Feng, H., 2023. PRMT6 inhibits K63-linked ubiquitination and promotes the degradation of IRF3 in the antiviral innate immunity of black carp Mylopharyngodon piceus. Aquaculture 562, 738872. https://doi.org/10.1016/j.aquaculture.2022.738872.

Yang, X., Ai, Y., Chen, L., Wang, C., Liu, J., Zhang, J., Li, J., Wu, H., Xiao, J., Chang, M., Feng, H., 2023. PRKX down-regulates TAK1/IRF7 signaling in the antiviral innate immunity of black carp Mylopharyngodon piceus. Front. Immunol. 13, 999219 https://doi.org/10.3389/fimmu.2022.999219.